Mid-infrared light emission from a Fe^{2+}:ZnSe polycrystal using quantum cascade laser pumping

Yu Song,[1,a)] Jens Sonntag,[1,b)] Sergey B. Mirov,[2] Claire F. Gmachl,[1] and Jacob B. Khurgin[3]
[1]*Department of Electrical Engineering, Princeton University, Princeton, New Jersey 08540, USA*
[2]*Department of Physics, University of Alabama at Birmingham, 421 Campbell Hall, 1300 University Blvd., Birmingham, Alabama 35294, USA*
[3]*Department of Electrical and Computer Engineering, Johns Hopkins University, Baltimore, Maryland 21218, USA*

(Received 2 August 2014; accepted 27 September 2014; published online 8 October 2014)

We report the realization of light emission from a Fe^{2+} doped ZnSe polycrystal with efficient pumping from a quantum cascade (QC) laser. The QC laser photon energy is near the absorption edge of the Fe^{2+}:ZnSe with less than ~60 meV Stokes' shift. The Fe^{2+}:ZnSe polycrystal shows an absorption band of ~2.2 – 5 μm in the mid-infrared (mid-IR) at room temperature, which narrows down to ~2.4–4.2 μm at 80 K. Clear photoluminescence (PL) from 4.5 μm to 6 μm are observed throughout the temperature range of 300 K to 80 K. At room temperature, the luminescence lifetime is about 0.38 ± 0.1 μs which increases up to 101 ± 2 μs at 118 K. This system transfers energy stored in the upper state of a QC laser with ~ps lifetime to the Fe^{2+}:ZnSe with 10^5 to 10^8 times longer lifetime, at the cost of minute photon energy losses. © *2014 AIP Publishing LLC*.
[http://dx.doi.org/10.1063/1.4897546]

With significant progress made in the past two decades, mid-infrared (mid-IR) quantum cascade (QC) lasers nowadays display many merits including a wide and continuous range of operating wavelengths,[1–3] high output power,[4–6] high efficiency,[7–9] and excellent temperature characteristics,[10,11] and they have been widely employed in a variety of applications.[12–14] However, it is still challenging to achieve mode locking or Q-switching in QC lasers, due to their intrinsic fast carrier re-distribution and gain recovery lifetimes.[15–18] This limits their applications in areas where ultrafast and high peak power operation is required, e.g., laser surgery, remote sensing of trace molecules, etc. In the near-IR, it is routine to use solid state (or fiber) pumped by laser diodes to achieve high peak power and short pulses. Here, we intend to extend this practice to the mid-IR. With long gain recovery lifetimes, the transition metal doped II-VI materials are a promising solid state gain medium in the mid-IR,[19–22] especially for their capability of ultra high peak power operation[23–25] and the added benefit of broad tunability.[26–28] However, the conventional pumping sources of these materials have mostly been several stages of diode, fiber and/or other solid state lasers operating in the visible or near-IR range.[29–32] This leads to a complex and bulky system, with limited quantum efficiency due to a large energy difference in the pump and lasing photons. Consequently, the excessive heat dissipation has to be managed. Clearly, improvement in quantum efficiency and simplification of the system are highly desired.

In this work, we report the realization of mid-IR light emission from a Fe^{2+} doped ZnSe polycrystal gain medium with a QC laser as pumping source. Since the QC laser itself is an electrically pumped, compact semiconductor device, the entire setup is in a simple QC laser → Fe^{2+}:ZnSe "two stage" operation regime, which is expected to reduce the complexity of the mid-IR solid state light emitting system. Here, as a first step towards lasing operation, we investigate the photoluminescence (PL) characteristics of the Fe^{2+}:ZnSe crystal with the QC laser pumping source. Another advantage of QC lasers is their flexibility in the lasing wavelengths, which allows one to choose the pumping photon energy as close to that of the desired emission photons from the Fe^{2+}:ZnSe as possible, and in turn improve the quantum efficiency. Here, a QC laser with a photon energy less than 60 meV Stokes' shift from the the absorption edge of the Fe^{2+}:ZnSe is employed for demonstration.

The prospective laser medium studied in this work is a ZnSe polycrystal with a Fe^{2+} concentration of 1.5×10^{19} cm^{-3}. The sample is grown by the chemical vapor transport (CVT) technique in a sealed vacuumed ampoule.[29] After growth, Fe metal films are deposited on the surface of the polycrystal, and doping is accomplished through thermal diffusion. Then the sample is cut and polished into a rectangular slab with a thickness of 2.78 mm, the photo of which is shown in the lower right inset of Fig. 1.

The pumping laser used in this work is a high efficiency ultra-strong coupling QC laser.[33] For this experiment, the laser is operating at 80 K in pulsed mode, with a pulse width of 100 ns and a repetition rate of 80 kHz. The laser operates at a wavelength of 4.0 μm with a peak power of up to 3 W.

The schematic of the experimental setup for the PL study is shown in Fig. 1. Fourier Transform Infrared Spectrometry (FTIR) is used for recording the spectral characteristics of light emission from the Fe^{2+}:ZnSe. The polycrystal is mounted in a cryostat for temperature dependent measurements, with the PL emission fed into the FTIR through a ZnSe lens. The QC laser is mounted in a separate cryostat, the pumping light from which is focused onto the ZnSe polycrystal by again two ZnSe lenses. Since the

[a)]yusong@princeton.edu
[b)]Permanent address: Department of Physics, University of Duisburg-Essen, Duisburg, Germany.

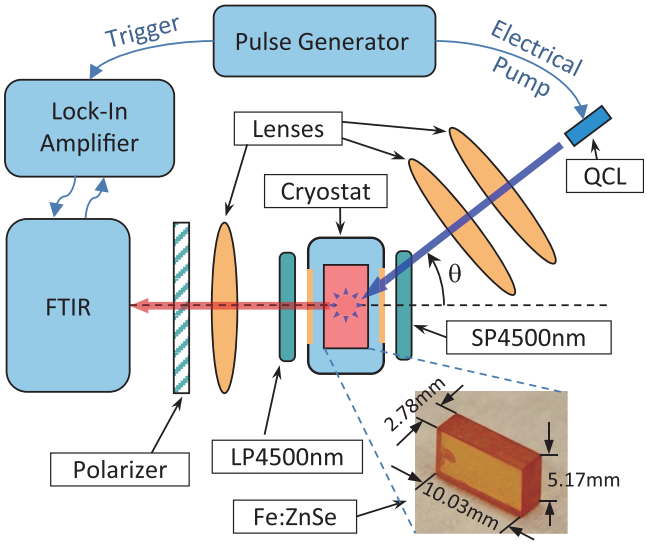

FIG. 1. Schematic of the experimental setup. The Fe^{2+}:ZnSe polycrystal is indicated in red rectangle inside the cryostat, with the photo shown in the lower right. Both the LP 4500 nm and the SP 4500 nm filters are placed against the ZnSe cryostat windows. All ZnSe lenses have a focal length of 1.5 in. The generated PL light is omnidirectional, but only a portion is collected into the FTIR.

residual and randomly scattered QC laser light is still several orders of magnitude stronger than the PL light and would easily saturate the Mercury Cadmium Telluride (MCT) detector of the FTIR, we use a long pass (LP) 4500 nm filter to quench the QC laser light after the polycrystal. A polarizer is also inserted in the optical path after the polycrystal, for further filtering of the QC laser light. The incidence angle θ as shown in Fig. 1 can be tuned from 0 to 45 degrees to avoid the straight transmitted pump light. A short pass (SP) 4500 nm filter is placed in front of the polycrystal to eliminate any incoming ambient light noise at longer wavelengths. A lock-in amplifier is used to collect the PL signal.

A similar setup is used for studying the time resolved PL (TRPL) characteristics at different temperatures. The FTIR is now replaced by a sensitive MCT detector in the TRPL measurements, the signals of which are recorded by a fast boxcar-oscilloscope.

The transmission spectra of the Fe^{2+}:ZnSe polycrystal from room temperature to cryogenic temperature are shown in Fig. 2. A wide absorption band in the mid-IR wavelength range is clearly seen in the figure. At room temperature, it covers a range of about 2.2 μm–5 μm, which significantly narrows down to about 2.4 μm–4.2 μm at 80 K. The wavelength of the pumping laser is also marked in the figure at 4.0 μm, which is near the edge of the absorption band with a stokes shift of about 60 meV at 300 K and only about 10 meV at 80 K. Throughout the full temperature range from 80 K to 300 K, 4 μm is constantly contained in the wavelength range of the Fe^{2+}:ZnSe emission cross section with effective pumping.[29,34] Thus, in this demonstration, the energy loss between the pumping and emission photons is minimal. A schematic energy diagram is also shown in the inset of Fig. 2.

The PL spectra of the Fe^{2+}:ZnSe polycrystal with QC laser pumping are plotted in Fig. 3. Light emission is clearly observed across the temperature range from 80 K to 300 K.

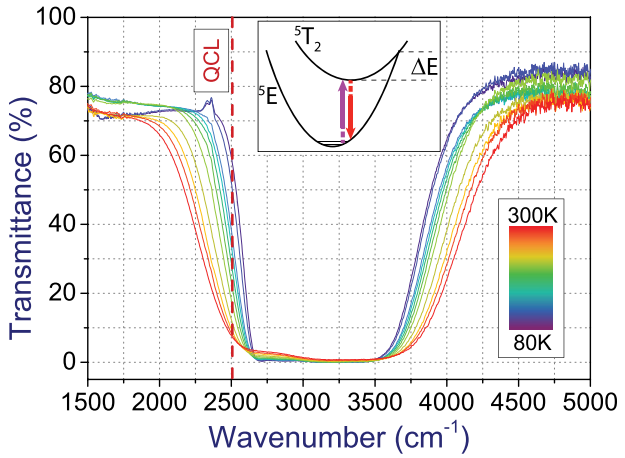

FIG. 2. Transmission spectra of the Fe^{2+}:ZnSe polycrystal at varying temperatures from 80 K to 300 K. The red dashed line indicates the wavelength of the pumping laser. Baseline of transmission is between 70%–80% due to surface reflection. At 300 K, about 60% of the pumping laser light is absorbed in the polycrystal, whereas, at 80 K, the absorbance is about 10% due to the narrowing of the absorption band. Inset: a schematic energy diagram. ΔE is the activation energy. Purple and red arrows indicate the pumping and emission optical transitions.

Since a LP 4500 nm filter is inserted in the optical path to quench the residual laser light, the recorded PL spectra are also partially blocked by the filter. While the emission cross section of the polycrystal is expected to be centered around 4.1 μm,[34] only the part beyond 4.5 μm is shown in Fig. 3, which reaches as far as 6 μm on the long wavelength side. In the normalized PL spectra shown in the inset of Fig. 3, a clear narrowing at lower temperatures is discernable, aside from a better signal-to-noise ratio. This is due to the narrowing of the emission cross section.[34] As is shown in Fig. 3, the PL intensity dramatically increases as temperature is reduced, reaches a peak at around 180 K, and then decreases again. This is a combined effect of three causes: the increase of the absolute PL intensity at lower temperatures; the narrowing of the PL peak at lower temperatures, effectively moving away from the recorded wavelength range; and the reduction in the absorbed pumping power at lower

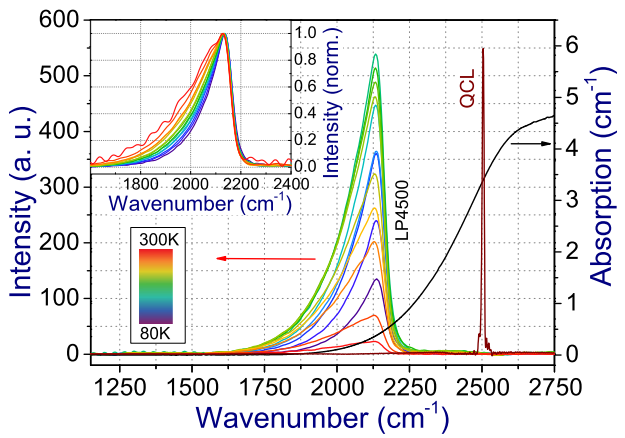

FIG. 3. PL spectra of the Fe^{2+}:ZnSe polycrystal at different temperatures with QC laser pumping shown in the solid curves in rainbow color. The PL spectra are plotted in the absolute scale in arbitrary yet comparable units. The absorption spectrum at 300 K (black) and the QC laser emission spectrum (dark red) are also plotted. Inset: normalized PL spectra.

temperatures due to the narrowing of the absorption band as shown in Fig. 2.

The TRPL measurement results are plotted in Fig. 4. The luminescence intensity from the polycrystal under delta pumping is expected to decay exponentially over time with a characteristic lifetime τ, which depends on the temperature. In these measurements, since the pumping laser photon energy is close to that of the emitted luminescence photons, the intra-manifold relaxation time is short. And the luminescence lifetime τ is dominated by the inter-manifold optical transition and the non-radiative recombination.[28] The MCT detector employed here has the advantage of high sensitivity, yet the time response is relatively slow. In the inset of Fig. 4, the detector response function to a delta pumping pulse (100 ns) from a QC laser is plotted in the green curve, which is as long as a few μs. Thus, the luminescence signal readout in the MCT detector is the convolution of the actual decaying luminescence intensity and the detector response function. Examples of the recorded PL signal at 300 K and 80 K are also plotted in the inset. The PL signal can be de-convolved and fitted with the detector response function to retrieve the luminescence lifetime τ, and the results are plotted in Fig. 4 as a function of temperature. The fitted PL signals are overlapped with the experimental data in the inset of Fig. 4. At 300 K, a delay and broadening in the PL signal vs. the detector response is discernable, which arises due to the relatively slow decaying PL light compared to the 100 ns pumping pulse. The luminescence lifetime increases significantly as the temperature drops down, and the PL signal at 80 K shows a shape of purely exponential decay, as seen in Fig. 4. The luminescence lifetime increases from 0.38 ± 0.01 μs at 300 K to 101 ± 2 μs at 118 K. The decrease of the luminescence lifetime below 118 K to $\sim$97 μs arises due to magnetic Fe^{2+}–ZnSe interactions.[35] These values of lifetimes are close to what have been reported in Refs. 28, 29, 34, and 35, where

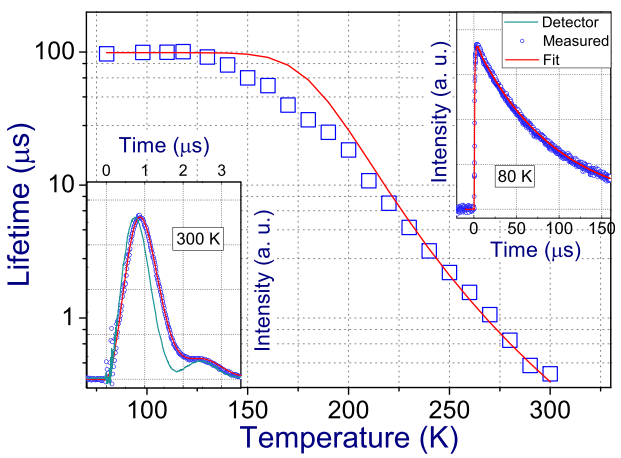

FIG. 4. Measured (blue squares) and fitted (red curve) luminescence lifetimes of Fe^{2+}:ZnSe polycrystal with the QC laser pumping at different temperatures. Insets: the detector response (green); the PL signals recorded by MCT detectors (blue circles); and the fitted PL signals (red), at 300 K (left inset) and 80 K (right inset). Time is referenced at the onset of the 100 ns pumping pulse. Note the difference in the time scales in the two inset figures. At 300 K, the luminescence lifetime and the detector response time are on the same order of magnitude, and the PL lifetime is deconvoluted from the total response curve. At 80 K, the luminescence lifetime is two orders of magnitude longer than the detector response time, and the line shape is dominated by the exponential decay.

significantly shorter wavelength pumping sources are used. Thus with a QC laser pumping source, the luminescence lifetime in Fe^{2+}:ZnSe is $10^5 \sim 10^8$ times longer than that of the QC lasers themselves. The measured temperature dependence of the luminescence lifetime can be fitted to estimate the activation energy ΔE according to[36]

$$\tau^{-1} = \tau_{rad}^{-1} + W_0 e^{-\Delta E/kT}, \quad (1)$$

where τ and τ_{rad} are the measured and radiative luminescence lifetime, respectively. W_0 is a constant. The fitted curve is plotted in Fig. 4, with $\Delta E = 241$ meV and $1/W_0 = 30$ ps, again in good agreement with those reported in literatures.[28,35]

In conclusion, we have demonstrated light emission from a Fe^{2+}:ZnSe polycrystal with a QC laser as pumping source, which is a major step towards the realization of QCL pumped solid state mid-IR lasers. The QC laser emits at 4 μm, which is located at the edge of the Fe^{2+}:ZnSe absorption band and in the middle of the emission cross section, i.e., with a small Stokes' shift. Photoluminescence from the Fe^{2+}:ZnSe polycrystal is observed across the temperature range from 300 K to 80 K, and the emission spectra from 4.5 μm to 6 μm are recorded. The PL lifetime studied with the TRPL measurements reads 0.38 ± 1 μs at 300 K, and reaches a peak of 101 ± 2 μs at 118 K. The light emission system transfers energy stored in the upper state of the QC laser to the upper manifold in the Fe^{2+}:ZnSe gain medium with 10^5–10^8 times longer scattering lifetime, with minimum photon energy loss. Future work shall focus on obtaining laser operation in the Fe^{2+}:ZnSe polycrystal with QC laser pumping. To this end, optical feedback from a properly designed cavity is needed. Mode-locking operation is also anticipated with the usage of Kerr lensing, semiconductor saturable absorber mirrors, etc.[23,37] Due to the fact that QC lasers are electrically pumped, compact semiconductor light sources with engineerable wavelengths in the mid-IR, reduction in the overall system complexity, easier thermal management and improvement over quantum efficiency are expected, alongside with ultra short pulses and high peak power in the mode locking operation.

This work was supported, in part, by MIRTHE, a NSF Engineering Research Center at Princeton and partners.

[1]M. Razeghi, N. Bandyopadhyay, Y. Bai, Q. Lu, and S. Slivken, Opt. Mater. Express **3**, 1872 (2013).
[2]A. Bismuto, S. Riedi, B. Hinkov, M. Beck, and J. Faist, Semicond. Sci. Technol. **27**, 045013 (2012).
[3]D. Chastanet, G. Lollia, A. Bousseksou, M. Bahriz, P. Laffaille, A. N. Baranov, F. Julien, R. Colombelli, and R. Teissier, Appl. Phys. Lett. **104**, 021106 (2014).
[4]Q. Y. Lu, Y. Bai, N. Bandyopadhyay, S. Slivken, and M. Razeghi, Appl. Phys. Lett. **98**, 181106 (2011).
[5]F. Xie, C. Caneau, H. LeBlanc, D. Caffey, L. Hughes, T. Day, and C. en Zah, in *23rd IEEE International Semiconductor Laser Conference (ISLC), 2012* (IEEE, 2012), pp. 32–33.
[6]J. C. Zhang, F. Q. Liu, D. Y. Yao, N. Zhuo, L. J. Wang, J. Q. Liu, and Z. G. Wang, J. Appl. Phys. **113**, 153101 (2013).
[7]Y. Bai, N. Bandyopadhyay, S. Tsao, S. Slivken, and M. Razeghi, Appl. Phys. Lett. **98**, 181102 (2011).
[8]R. Maulini, A. Lyakh, A. Tsekoun, and C. K. N. Patel, Opt. Express **19**, 17203 (2011).

[9]B. Hinkov, A. Bismuto, Y. Bonetti, M. Beck, S. Blaser, and J. Faist, Electron. Lett. **48**, 646 (2012).
[10]P. Laffaille, J. C. Moreno, R. Teissier, M. Bahriz, and A. N. Baranov, AIP Adv. **2**, 022119 (2012).
[11]K. Fujita, M. Yamanishi, S. Furuta, A. Sugiyama, and T. Edamura, Appl. Phys. Lett. **101**, 181111 (2012).
[12]W. Ren, W. Jiang, N. P. Sanchez, P. Patimisco, V. Spagnolo, C.-e. Zah, F. Xie, L. C. Hughes, R. J. Griffin, and F. K. Tittel, Appl. Phys. Lett. **104**, 041117 (2014).
[13]R. Martini and E. Whittaker, J. Opt. Fiber Commun. Rep. **2**, 279 (2005).
[14]S. Liakat, K. A. Bors, T.-Y. Huang, A. P. M. Michel, E. Zanghi, and C. F. Gmachl, Biomed. Opt. Express **4**, 1083 (2013).
[15]A. Hugi, G. Villares, S. Blaser, H. C. Liu, and J. Faist, Nature **492**, 229 (2012).
[16]A. K. Wójcik, P. Malara, R. Blanchard, T. S. Mansuripur, F. Capasso, and A. Belyanin, Appl. Phys. Lett. **103**, 231102 (2013).
[17]K. Maussang, J. Maysonnave, N. Jukam, J. R. Freeman, P. Cavalié, S. P. Khanna, E. H. Linfield, A. G. Davies, H. E. Beere, D. A. Ritchie, S. S. Dhillon, and J. Tignon, AIP Conf. Proc. **1566**, 504 (2013).
[18]J. B. Khurgin, Y. Dikmelik, A. Hugi, and J. Faist, Appl. Phys. Lett. **104**, 081118 (2014).
[19]S. B. Mirov, V. V. Fedorov, D. V. Martyshkin, I. S. Moskalev, M. S. Mirov, and V. P. Gapontsev, Opt. Mater. Express **1**, 898 (2011).
[20]G. Feng, C. Yang, and S. Zhou, Nano Lett. **13**, 272 (2013).
[21]J. W. Evans, P. A. Berry, and K. L. Schepler, Opt. Lett. **37**, 5021 (2012).
[22]A. Godard, C. R. Phys. **8**, 1100 (2007).
[23]J. Evans, P. Berry, and K. Schepler, IEEE J. Quantum Electron. **50**, 204 (2014).
[24]N. Myoung, D. V. Martyshkin, V. V. Fedorov, and S. B. Mirov, Opt. Lett. **36**, 94 (2011).
[25]J. Kernal, V. V. Fedorov, A. Gallian, S. B. Mirov, and V. V. Badikov, Opt. Express **13**, 10608 (2005).
[26]M. Doroshenko, H. Jelínková, P. Koranda, J. Šulc, T. Basiev, V. Osiko, V. Komar, A. Gerasimenko, V. Puzikov, V. Badikov, and D. Badikov, Laser Phys. Lett. **7**, 38 (2010).
[27]V. I. Kozlovsky, V. A. Akimov, M. P. Frolov, Y. V. Korostelin, A. I. Landman, V. P. Martovitsky, V. V. Mislavskii, Y. P. Podmar'kov, Y. K. Skasyrsky, and A. A. Voronov, Phys. Status Solidi B **247**, 1553 (2010).
[28]V. Fedorov, S. Mirov, A. Gallian, D. Badikov, M. Frolov, Y. Korostelin, V. Kozlovsky, A. Landman, Y. Podmar'kov, V. Akimov, and A. Voronov, IEEE J. Quantum Electron. **42**, 907 (2006).
[29]S. Mirov, V. Fedorov, I. Moskalev, D. Martyshkin, and C. Kim, Laser Photonics Rev. **4**, 21 (2010).
[30]V. Fedorov, A. Gallian, I. Moskalev, and S. Mirov, J. Lumin. **125**, 184 (2007), festschrift in Honor of Academician Alexander A. Kaplyanskii.
[31]M. P. Frolov, Y. V. Korostelin, V. I. Kozlovsky, V. V. Mislavskii, Y. P. Podmar'kov, S. A. Savinova, and Y. K. Skasyrsky, Laser Phys. Lett. **10**, 125001 (2013).
[32]E. Sorokin, S. Naumov, and I. Sorokina, IEEE J. Sel. Top. Quantum Electron. **11**, 690 (2005).
[33]P. Q. Liu, A. J. Hoffman, M. D. Escarra, K. J. Franz, J. B. Khurgin, Y. Dikmelik, X. Wang, J.-Y. Fan, and C. F. Gmachl, Nat. Photonics **4**, 95 (2010).
[34]J. J. Adams, C. Bibeau, R. H. Page, D. M. Krol, L. H. Furu, and S. A. Payne, Opt. Lett. **24**, 1720 (1999).
[35]N. Myoung, V. V. Fedorov, S. B. Mirov, and L. E. Wenger, J. Lumin. **132**, 600 (2012).
[36]B. Henderson and R. H. Bartram, *Crystal-field Engineering of Solid-state Laser Materials* (Cambridge University Press, 2005), Vol. 25.
[37]M. N. Cizmeciyan, H. Cankaya, A. Kurt, and A. Sennaroglu, Opt. Lett. **34**, 3056 (2009).